We are IntechOpen,
the world's leading publisher of
Open Access books
Built by scientists, for scientists

4,800
Open access books available

122,000
International authors and editors

135M
Downloads

Our authors are among the

154
Countries delivered to

TOP 1%
most cited scientists

12.2%
Contributors from top 500 universities

CLARIVATE ANALYTICS
BOOK CITATION INDEX
INDEXED

WEB OF SCIENCE™

Selection of our books indexed in the Book Citation Index
in Web of Science™ Core Collection (BKCI)

Interested in publishing with us?
Contact book.department@intechopen.com

Numbers displayed above are based on latest data collected.
For more information visit www.intechopen.com

A Density Functional Theory Study of Chemical Functionalization of Carbon Nanotubes - Toward Site Selective Functionalization

Takashi Yumura

Department of Chemistry and Materials Technology, Kyoto Institute of Technology,
Matsugasaki, Sakyo-ku, Kyoto
Japan

1. Introduction

Single walled carbon nanotubes exhibit metallic or semiconducting characters, depending on how to roll-up graphene sheet (Iijima, 1991; Iijima & Ichihashi, 1993; Dresselhaus et al., 1996; Saito et al., 1998). In addition of the unique electronic properties, functionalization of nanotubes can expand the versatility because of enhancing their solubility as well as feature expansion by attached functional groups (Hirsch, 2002; Haddon, 2002; Niyogi et al., 2002; C.A. Dyke & Tour, 2004; Tasis et al., 2006; Prato et al, 2008; Vzquez & Prato, 2009; Strano et al., 2009; Karousis et a;., 2010). The functionalization is roughly categorized into two types; noncovalent- and covalent-functionalization. In covalent functionalization, only highly reactive reagents are available. In a pioneering paper discussing the covalent bond formation, Haddon et al. reported that nanotubes were successfully functionalized by a divalent carbene-derivative CCl_2 (Chen et al., 1998; Chen et al., 1998; Kamarás et al., 2003). In the experiments, its divalent atom binds into two carbon atoms of a nanotube surface. After the publication, different types of cyclopropanized nanotube were generated by a single Bingel reaction (Coleman et al., 2003; Worsley et al., 2004; Umeyama et al., 2007). Note that Bingel reaction has been also utilized for selective functionalization of fullerenes (Diederich & Thilgen, 1996). Another type of covalent functionalization of nanotubes is radical additions. In this case, radical species, whose precursors are alkyhalides, diazonium salts, alky-lithium and so on, can make one covalent bond with a nanotube surface (Holzinger et al., 2001; Bahr & Tour , 2001; Bahr et al., 2001; Bahr et al., 2001; Ying et al., 2003; Saini et al., 2003; Peng et al., 2003; Stevens et al., 2003; Peng et al., 2003).

From a viewpoint of the electronic properties of nanotubes, covalent functionalization can modulate their band structures. If their bands in the vicinity of the Fermi level are significantly perturbed upon the functionalization, one can detect a sizable change of physically observable values, such as the conductivity. Recent theoretical studies evaluated the conductance of monovalent or divalent functionalized nanotubes (Park et al., 2006; Lee & Marzari, 2006; Lpez-Bezanilla et al., 2009). The theoretical findings suggested that divalent functionalization can preserve the conductance of its pristine nanotube, whereas monovalent case destroys it (Park et al., 2006; Lpez-Bezanilla et al., 2009). The theoretical

results inspired experimentalists to measure the conductance of functionalized nanotubes. In fact, changes of the conductance of nanotubes upon the functionalization were observed experimentally (Goldsmith et al., 2007; Kanungo et al., 2009).

Although our knowledge on functionalization of nanotubes has been expanded, "site-selective" functionalization in either divalent or monovalent manners has been still a challenging target in nanotube chemistry. The difficulty in achieving site selective functionalization comes from high reactivity of functional groups. Of course, higher reactive species are necessary to attach to a rigid tube-bond. In an opposed action they would attack randomly at almost equivalent tube-bonds. If one can control binding sites for carbene-derivatives on a nanotube surface to pattern the functional groups, such functionalization can open the door toward designing novel tube-based nanomachines. For example, Globus et al. proposed that "paddle wheels" can be constructed conceptually by addition of benzynes onto a nanotube circumferentially, whereas the addition in the axial direction results in "gear teeth" (Han & Globus, 1997; Globus et al., 1998). Accordingly, selective functionalization of nanotubes is now required to design the unique nanomachines.

For the purpose of achieving site-selective functionalization of nanotubes, it is indispensable to elucidate how functional groups interact with an outer or inner surface of a nanotube, as well as how the resultant interactions perturb its sp^2 bonding frameworks. In this direction, recent quantum chemistry calculations would help to obtain an insight of changes of nanotube surfaces upon the functionalization. In particular, recent advances in *ab initio* density functional theory (DFT) calculations, where Khon-Sham equations including electron correlation are solved iteratively (Hohenberg & Kohn, 1964; Kohn & Sham, 1965; Parr & Yang, 1996), allow us to accurately calculate large-scale systems like nanotubes. Enhancing the reliability of DFT calculations is due to improvement in the quality of exchange-correlation functionals (Becke, 1988; Lee et al., 1988; Becke, 1992; Becke, 1992; Becke, 1993; Stephens et al., 1994; Vosko et al., 1980). Actually, recent DFT methods can provide reliable data, such as energies and force in materials. Thus one can utilize the DFT calculations to look at CC bondings in nanotubes "on an atomic level", and to devise a plausible strategy toward site-selective functionalization of nanotubes.

Because of retaining the unique electronic properties of nanotubes after the divalent functionalization, we discuss in this chapter the properties of nanotubes functionalized by carbene-derivatives from a viewpoint of computational chemistry based on DFT calculations. The aim in this study is finding out an approach to how site-selective functionalization of nanotubes can be achieved. This chapter is organized as follows. In section 2.1, we briefly present how computational methods influence a description of its CC bonding network by investigating the addition of carbene into naphthalene as a simple test case. After the discussion, results of mono- or double functionalization of nanotubes are given. First, we discuss chemical reactivity of inner or outer tube surface toward carbene with the focus on surface modification by the addition in section 2.2. In sections 2.3, we propose two strategies for site-selective double addition into a nanotube, based on the findings in section 2.2. In section 2.3.1, we investigate whether surface modification induced by the inner carbene addition can direct the next carbene into a specific site. On the other hand, another strategy is introduced in section 2.3.2; the use of geometrical constraints of a bismalonate for site-selective addition into a nanotube. Finally we conclude this chapter in Section 3.

2.1 Choice of computational methods

Prior to discussing functionalization of nanotubes by carbene-derivatives, we briefly explain computational methods suitable to accurately describe the interactions. As a simple and relevant test case, we focused on the addition of carbene into naphthalene with ten π electrons (Choi & Kertesz, 1998). In the test case, we employed three different calculations; Hartree-Fock (HF), the second-order Møller-Plesset perturbation theory (MP2) (Szabo & Ostlund, 1996), and density functional theory (DFT) methods. In the DFT calculations, GGA-based PW91 functional and hybrid B3LYP functional are considered as a standard functional. When the divalent atom of carbene (labeled by C11) attacks at the bridgehead atoms of naphthalene (labeled by C1 and C6), the valence tautomerization of 1,6-methano[10]annulene occurs, as shown in the upper of Figure 1.
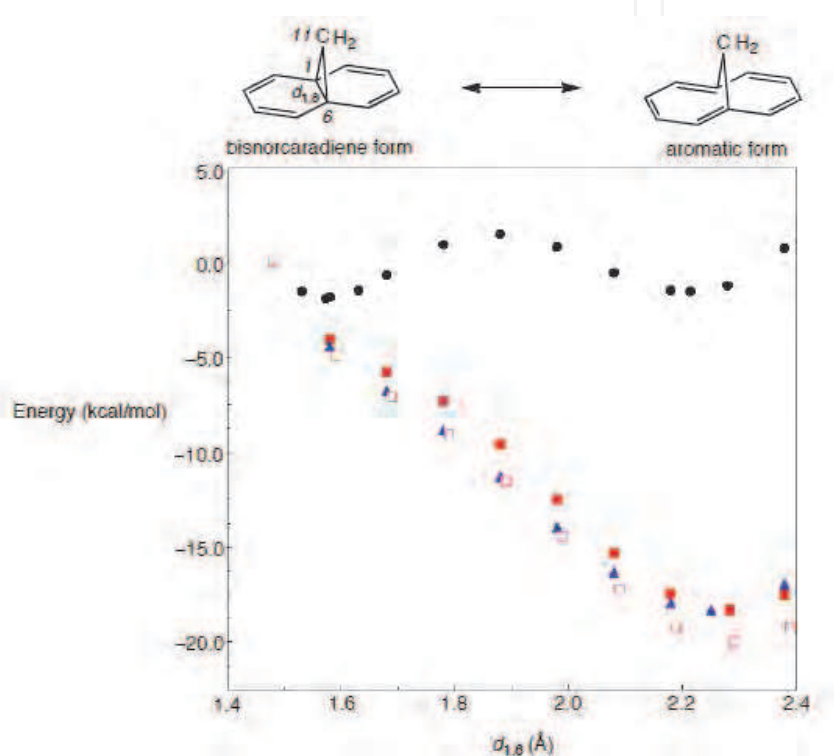

Fig. 1. Total energies of 1,6-methano[10]annulene as a function of the $d_{1,6}$ value, obtained from Hartree-Fock (black circles), second order Møller-Plesset perturbation theory (MP2) (blue triangles), and density functional theory calculations. PW91 and B3LYP functionals (purple open and red closed squares, respectively) are considered in the DFT calculations. The basis set used is the 6-31G* basis set.

In the tautomerization, there are two types of structure; one is bisnorcaradiene form, and the other is aromatic form. As shown in Figure 1, the two isomers can be distinguished by the separation between the C1 and C6 atoms (the $d_{1,6}$ bond); the bisnorcaradiene form has a shorter $d_{1,6}$ bond, whereas the aromatic form has a longer $d_{1,6}$ bond. Reflecting the $d_{1,6}$ values, the two tautomers have different number of π electrons in naphthalene-moiety. In the aromatic form, ten π electrons remain in its naphthalene-moiety, while two π electrons transfer from naphthalene to form two CC bonds in the bisnorcaradiene form.

The $d_{1,6}$ value is not only a geometrical parameter, but it is key in relative stability of the two tautomers of 1,6-methano[10]annulene. Figure 1 displays total energies of 1,6-methano[10]annulene against the $d_{1,6}$ value, depending on computational methods (HF,

MP2, and DFT (B3LYP and PW91 (Perdew & Wang, 1992) methods). As shown in Figure 1, there are two local minima that are energetically equivalent in the HF calculations. The minima correspond to the bisnorcaradiene and aromatic forms. However, we obtained from DFT and MP2 calculations only an aromatic form as a stable conformation. The calculated $d_{1,6}$ values are around 2.3 Å, which can reproduce that obtained experimentally (2.235 Å) (Bianchi et al., 1980). The DFT and MP2 methods include electron correlation, but the HF method does not include. Thus, the differences indicate that electron correlation should be important in relative stability of the two tautomers, and describing the geometrical change of naphthalene induced by the interactions with carbene.

In general, MP2 calculations are more time-consuming than DFT calculations. Since nanomaterials, such as nanotubes, contain few hundred of atoms in the unit cell, MP2 methods are not doable to estimate the properties of nanomaterials. Actually our systems introduced in this chapter contain up to 240 carbon atoms of a nanotube plus a few functional groups in the unit cell in periodic boundary condition (PBC) calculations. Instead, DFT methods, which can describe their properties in a relatively accurate manner, are less time-consuming. Accordingly, we will investigate interactions between carbene-derivatives and a nanotube surface by using DFT methods with B3LYP or PW91 functionals.

2.2 Addition of carbene into a nanotube, and concomitant surface modification

Let us first discuss the addition of carbene into the outer (Chen et al., 2004; Bettinger, 2004; Zhao et al., 2005; Bettinger, 2006; Zheng et al., 2006; Yumura & Kertesz, 2007; Yumura et al., 2007; Lee & Marzari, 2008) or inner (Yumura & Kertesz, 2007; Yumura et al., 2007) surface of the (5,5) or (10,10) nanotube, whose optimized geometries are seen in Figures 2 and 3.

As mentioned above, the divalent atom of carbene binds into a CC bond of sp^2 systems. The (5,5) and (10,10) nanotubes have two types of CC bond (a CC bond orthogonal or slanted relative to the tube axis). Accordingly, there are two types of optimized structure for an inner (outer) carbene binding into an armchair nanotube. Figures 2 and 3 show the preferences of an orthogonal site over a slanted site as the single carbene addition, irrespective of an inner or outer addend. In terms of the geometrical features, a slanted bond retains after the addition of an inner or outer carbene, as shown in Figures 2 and 3 (Yumura & Kertesz, 2007; Yumura et al., 2007). When carbene binds into an orthogonal site, different behaviors were found between the inner and outer surfaces. The inner addition retains the orthogonal bond, whereas the outer addition breaks it. The different behaviors come from more rigorous restriction of surface modification toward the tube center. This is understandable from a strain analysis based on π-orbital axial vector (POAV) (Haddon, 1998), where the strain energy is proportional to the square of a POAV value. In fact, a POAV value would increase by the surface modification toward the center. Then the strain energy would be more pronounced, if carbene freely binds into the inner surface rather than into the outer surface. As a result, the concave nanotube surface prohibits inner carbene from freely binding into the inner surface to keep the CC bond at the binding site.

Breaking or retaining the CC bond at the binding site of a nanotube is reminiscent of the valence tautomerization of 1,6-methano[10]annulene. From an analogy to 1,6-methano[10]annulene whose tautomers have different number of π electrons, we can understand the modification of a nanotube upon the carbene addition obtained from DFT

A Density Functional Theory Study of Chemical Functionalization
of Carbon Nanotubes - Toward Site Selective Functionalization
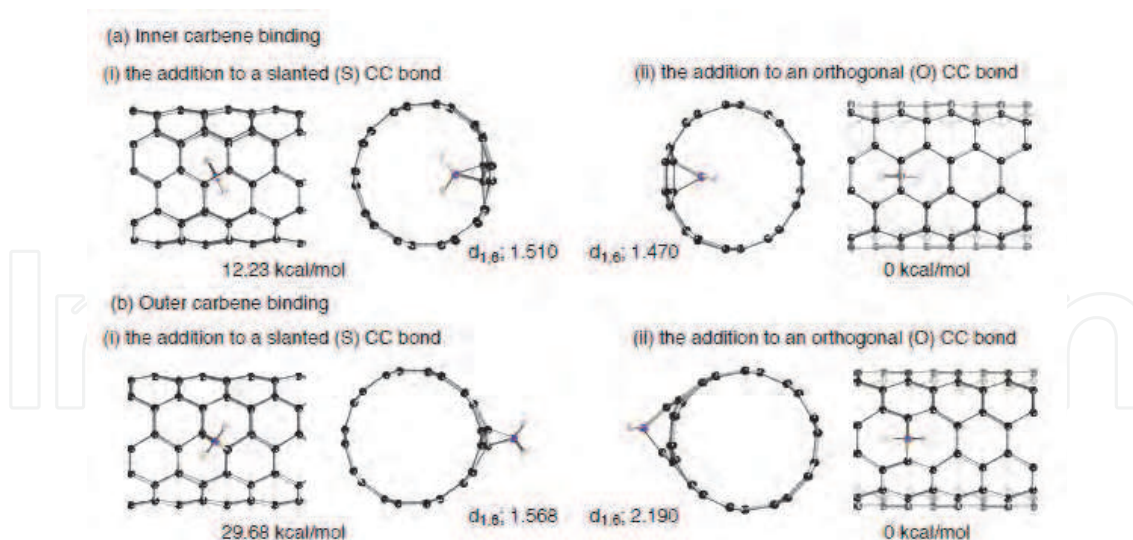
313

Fig. 2. Optimized structures for the addition of carbene into an inner or outer surface of the (5,5) nanotube. Their relative energies are also given in kcal/mol, lengths of the CC bond at the binding site (the $d_{1,6}$ values) in Å. These values were obtained from PW91 PBC calculations (Yumura & Kertesz, 2007).
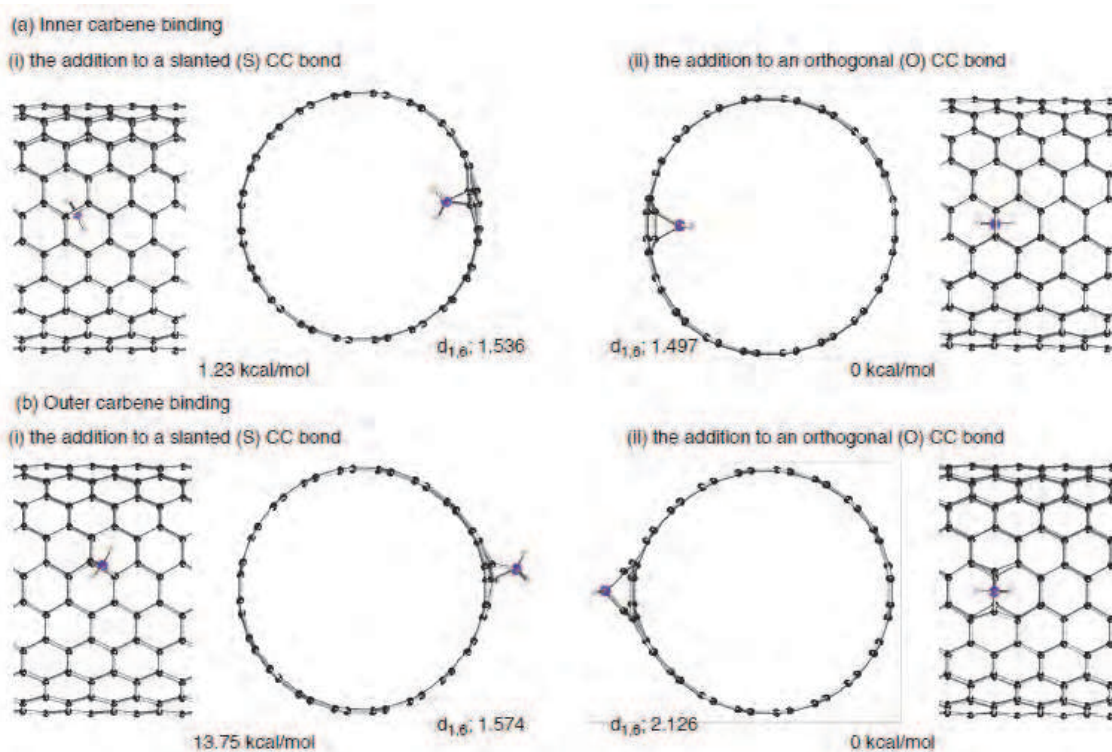

Fig. 3. Optimized structures for the addition of carbene into an inner or outer surface of the (10,10) nanotube. Their relative energies are also given in kcal/mol, lengths of the CC bond at the binding site (the $d_{1,6}$ values) in Å. These values were obtained from PW91 PBC calculations (Yumura et al., 2007).

calculations. To interpret the surface modification, we applied a basic concept in organic chemistry, the Clar concept (Clar, 1972). Based on Clar valence bond (VB) representation, all π electrons in the pristine armchair nanotubes can be given by aromatic sextet (Matsuo et al.,

2003; Ormsby & King, 2004; Ormsby & King, 2007). In the inner addition into a nanotube where the $d_{1,6}$ CC bond retains, two π electrons migrate from the nanotube. Due to the π electron migration, the CC bondings of the nanotube attached by inner carbene are significantly perturbed. Based on the Clar representation, the perturbed surface consists of two butadiene (B) patterns near the binding site plus quinonoid (Q) pattern in the circumferential direction (Figure 4(a)).
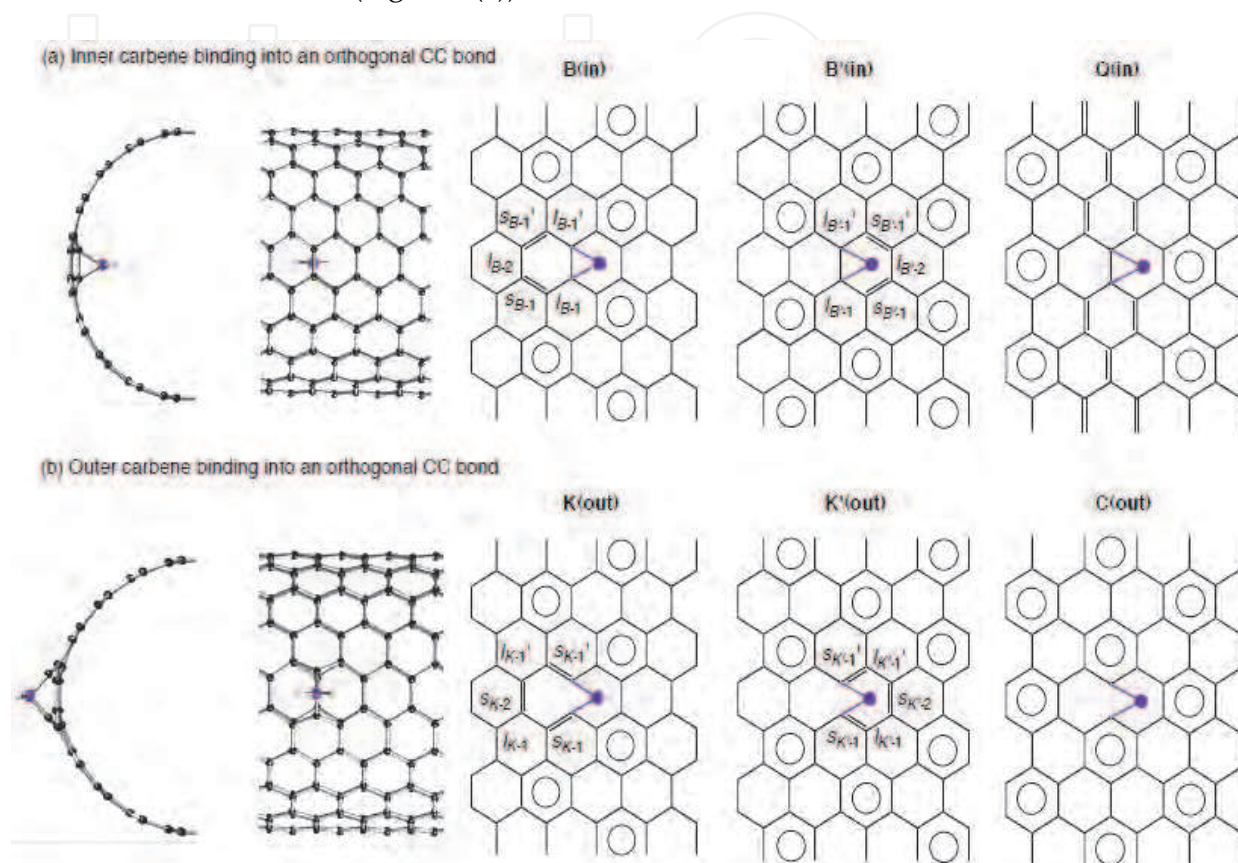

Fig. 4. Clar representation of modified nanotube surface upon the functionalization by inner (a) or outer (b) carbene. Aromatic sextets are given by circles. Note that pristine armchair nanotubes have all π electrons represented by aromatic sextets.

Basically, the DFT-optimized geometries for the nanotubes attached by inner CH_2 are explainable from the Clar representation, as shown in Table 1 and Figure 5. Actually, bond-length alternations in the circumferential direction follow the Q pattern in Figure 5, but the alternations are significant only near the binding site. Similar perturbation patterns can be seen in a defected nano-peapod (Figure 6) where a defected C_{60} (C_1-C_{59}) makes two covalent bonds with the inner surface of the (10,10) nanotube (Yumura et al., 2007). Intrinsic reaction coordination (IRC) analyses based on B3LYP calculations suggest that C_{60} directly converts into a C_1-C_{59} defect as the initial intermediate with a barrier of 8.4 eV (Yumura et al., 2007). Experimentally, the formation of defective fullerenes has been actually observed under electron irradiation in transmission electron microscopy measurements (TEM) (Urita et al., 2004; Sato et al., 2006). Thus, one can utilize the activation of guest molecules (e.g. by heating-treatment or electron irradiation) to locally perturb a host nanotube surface from inside out.

	l_{B-1}	s_{B-1}	l_{B-2}	s_{B-1}'	l_{B-1}'	$l_{B'-1}$	$s_{B'-1}$	$l_{B'-2}$	$s_{B'-1}'$	$l_{B'-1}'$
(5,5)	1.471	1.402	1.470	1.402	1.471	1.470	1.403	1.471	1.401	1.470
(10,10)	1.468	1.399	1.454	1.399	1.468	1.469	1.399	1.454	1.398	1.469

Table 1. Optimized bond-lengths (Å) within the two six-membered rings nearest to the site for the binding of inner carbene along the axis of a (5,5) or (10,10) tube according to PW91 PBC calculations. Definition of bond types is given in Figure 4.
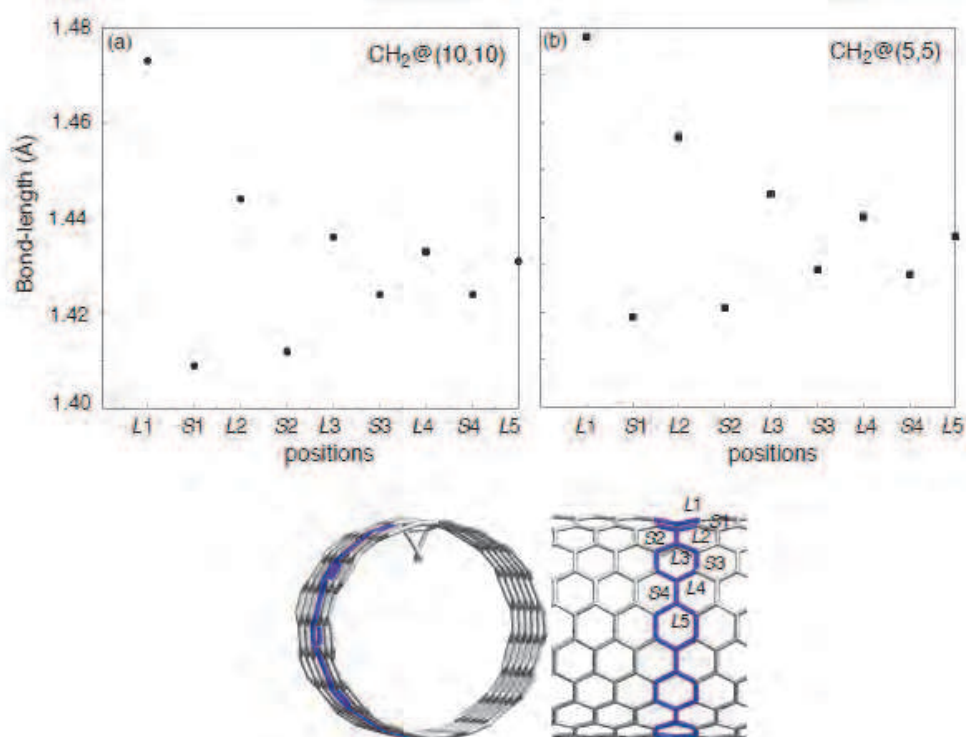

Fig. 5. Bond length alternations of quinonoid patterns in the circumferential direction of the (5,5) or (10,10) nanotube functionalized by inner carbene. The bond lengths were obtained from PW91 PBC calculations. L and S indicate longer and shorter bonds in the quinonoid pattern in Figure 4, respectively (Yumura & Kertesz, 2007; Yumura et al., 2007).

In contrast, the outer carbene addition cleaves the $d_{1,6}$ CC bond at an orthogonal site. In this situation, π electrons do not migrate, instead σ electrons participate in the formation of the new covalent bonds. As a result, Clar patterns of the nanotube remain almost unchanged after the outer addition, except for the two six-membered rings nearest to the binding site in the axial direction, where Kekulé patterns appear (Table 2). The surface modification patterns in the inner or outer carbene additions are completely different from those in the alkyl radical. additions (Yumura, 2011). In the outer radical additions, D_{3h}-like deformation patterns appear due to the formation of one covalent bond. In contrast, an inner radical prefers energetically to separate from a tube rather than to form one covalent bond together with modifying the surface structure. This result indicates the inertness of the inner surface of a nanotube, because the destabilization due to the surface modification dominates the stabilization due to the weak covalent bond formation. Lower reactivity of inner surface toward H or F atom than outer surface was also reported Chen et al. (Chen et al., 2003)
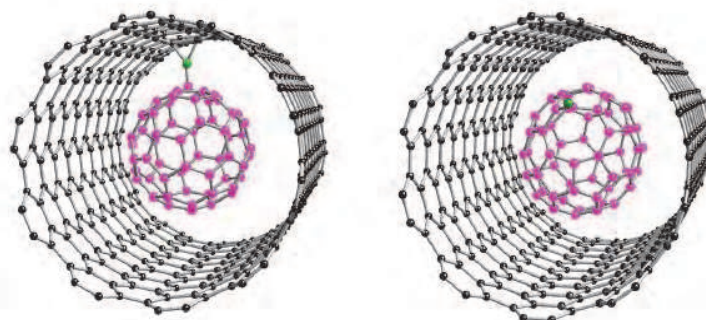
Fig. 6. Two types of optimized geometry for defected nanopeapod (C_1-C_{59}@(10,10) tube). Two covalent bonds are formed between a defected fullerene (C_1-C_{59}) and the nanotube in the left-hand side compound, whereas the right-hand side compound does not have such inner covalent bonds. The reactive C_1 atom in the defected fullerene is given by green, and the C_{59} moiety by purple. The optimized structures were obtained from PBC PW91 calculations (Yumura et al., 2007) as well as a B3LYP cluster approach (Yumura et al., 2007).

	$s_{K\text{-}1}$	$l_{K\text{-}1}$	$s_{K\text{-}2}$	$l_{K\text{-}1}'$	$s_{K\text{-}1}'$	$s_{K'\text{-}1}$	$l_{K'\text{-}1}$	$s_{K'\text{-}2}$	$l_{k'\text{-}1}'$	$s_{K'\text{-}1}'$
(5,5)	1.414	1.451	1.444	1.452	1.410	1.410	1.451	1.444	1.452	1.411
(10,10)	1.414	1.444	1.448	1.445	1.415	1.414	1.445	1.448	1.445	1.413

Table 2. Optimized bond-lengths (Å) within the two six-membered rings nearest to the site for the binding of outer carbene along the axis of a (5,5) or (10,10) tube according to PW91 PBC calculations. Definition of bond types is given in Figure 4.
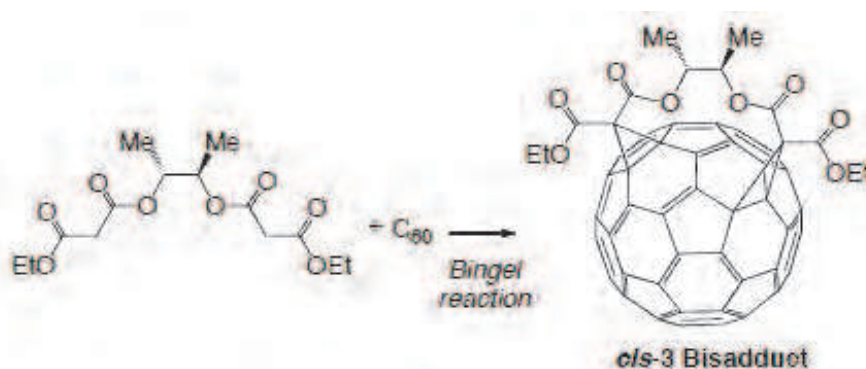
2.3 Site-selective double additions

Considering the surface modification created by the single carbene addition, let us devise plausible strategies for enhancing site-selectivity of double divalent additions. The CC bonds in pristine nanotubes are nearly equivalent in terms of the length and electron density. Because of the featureless CC bonds in nanotubes, carbene derivatives cannot select a specific CC bond as a binding site. On the other hand, the inner carbene addition into a nanotube makes a great difference in the seamless sp² bondings; double- or single-bond characters appear only near the binding site. Thanks to increasing or decreasing electron population on CC bonds at the limited region, carbene can bind selectively into a CC bond with richer electron density. Therefore, "local" modification of a nanotube by the inner carbene addition can play an important role in site preferences for the second addition, as shown in Scheme 1 (Yumura & Kertesz, 2007). In this situation, we do not need to consider repulsion between the two carbenes.

Scheme 1

A Density Functional Theory Study of Chemical Functionalization
of Carbon Nanotubes - Toward Site Selective Functionalization

317

In contrast, such site-preferences for the addition of two outer carbenes into a nanotube are not expected. The most important reason is that a nanotube functionalized by outer carbene has Clar patterns plus Kekulé patterns only near the binding site. The double bonds in Kekulé patterns may be a good candidate for the binding site of the second carbene. However, the second carbene cannot add to a double CC bond of the six-membered rings with Kekulé patterns, because of repulsion between the two carbenes. Thus, conformational restrictions in functional groups with divalent atoms are necessary for site-selective functionalization of nanotubes. Here, we consider a bismalonate with a 2,3-butanediol tether as a functional group possible to bind selectively into a nanotube, drawing a direct line with fullerene chemistry reported by the Diderlich groups (Kessinger et al., 2000). Note that the bismalonate can selectively bind into fullerene to form only cis-3 adduction, as shown in Scheme 2.

Scheme 2

cis-3 Bisadduct

Thus, we investigate the addition of the bismalonate into a nanotube as another plausible approach (Yumura & Kertesz, 2009). In the following sections, we separately discuss the two strategies for the site-selective functionalization of nanotubes.

2.3.1 Cooperativity of double carbene additions

In this section, we discuss whether the surface modification induced by the first inner addition influences site-preferences for the second addition. To quantitatively look at the double addition (Scheme 1), two key values are the binding energy for the double additions ($E_{double-bind}$), and the interaction energy ($E_{interact}$), defined as follows,

$$E_{double-bind}(X) = E_{total}(C11(X)-NT-C11(0)) - E_{total}(NT) - E_{total}(substituent(s)) \qquad (1)$$

and

$$E_{interact}(X) = E_{double-bind}(X) - E_{single-bind}(X) - E_{single-bind}(0) \qquad (2)$$

where X and 0 represent sites for the second and first carbene bindings, respectively, and C11(X)–NT–C11(0) represents a nanotube attached by two divalent C11 atoms of carbenes or carbene-derivatives, and $E_{single-bind}(X)$ and $E_{single-bind}(0)$ are the binding energies for the single additions of the second and first carbenes, respectively. The interaction energy ($E_{interact}$) indicates how much the first addition can have the power to have an impact on site preferences for the second attachment through the concomitant surface modification. A negative (positive) $E_{interact}$ value indicates that the second addition into a site X is stabilized (destabilized) by the first inner addition. When two attached carbenes are far, the two carbenes do not exert influence each other. Accordingly, an $E_{interact}$ value would be negligible.

Here we estimated the $E_{double-bind}$ and $E_{interact}$ values at various sites for the second attachment after the first inner carbene addition into an orthogonal bond (Yumura & Kertesz, 2007). Considering the local modification by the first attachment, we choose possible sites (X) for the second binding site (Figure 7). We define an orthogonal binding site for the second CH_2 molecule (outer surface) as $O_p(q)$ relative to the binding site $O_0(0)$ for the first CH_2 molecule (inner surface). Here p represents the order of the carbon belt of $O_p(q)$ site, lying in a plane perpendicular to the axis, from the $O_0(0)$ site with respect to the armchair framework in the axial direction, and q represents the order of the orthogonal bond $O_p(q)$ with respect to the $O_0(0)$ site in the circumferential direction. In slanted binding sites, the $S_{p1-p2}(q)$ sites are between the p_1-st and p_2-nd carbon belts.
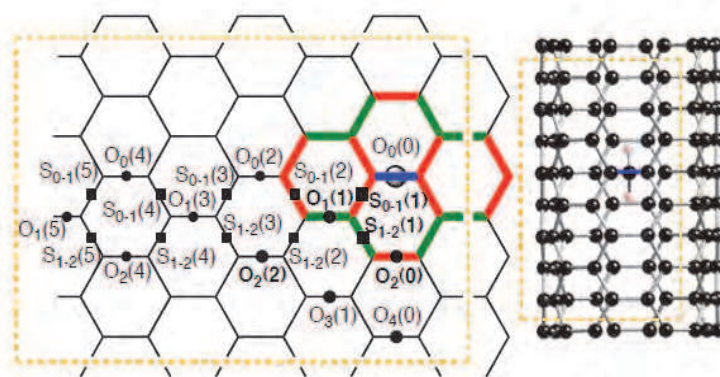

Fig. 7. Definition of sites for the second divalent C11 atom after the first divalent addition. The first addition site is given by $O_0(0)$. Based on Figure 4, double bond characters created by the first attachment are given by green, and single bond characters by red.

As a result of DFT calculations, we found that some configurations of the double addition have a negative $E_{interact}$ value (Yumura & Kertesz, 2007). The most noticeable $E_{interact}$ value was calculated at the $S_{1-2}(1)$ site to be around –25 kcal/mol. More importantly the effects of the first attachment on stabilizing the second attachment are limited near the first binding site. For example, energetically stable configurations in Figure 8 have significant $E_{interact}$ values ranging from –8.0 to –5.2 kcal/mol. Then the stabilized sites for second attachment have double-bond characters or are between double bonds. In other words, the second carbene attacks at a specific CC bond on which electron population enhances by the first attachment, as shown in Figures 4 and 7. The results strongly indicate cooperative behaviors between the first inner and second outer carbenes through the local surface modification. Thus DFT calculations demonstrate that the locally perturbed surface by the inner attachment, whose CC bond lengths change by up to 0.048 Å, has a strong impact of site-preferences for the second attachment.

Contrary, similar cooperative effects cannot be found between two carbenes binding into the outer surface of the (10,10) nanotube, based on DFT calculations (Yumura & Kertesz, 2009).

In the double outer additions, possible 20 sites for the binding of second carbene were considered. The $E_{doube-bind}$ and $E_{interact}$ values are plotted in Figure 9 as a function of the separation between the two divalent C11 atoms. As shown in Figure 9(a), we found that second orthogonal bindings are energetically favorable relative to slanted bindings, judging from the $E_{double-bind}$ values. Furthermore, DFT calculations found that four orthogonal sites have substantial $E_{interact}$ values with a negative sign in Figure 9(b) (–5.7 ~ –2.5 kcal/mol)

A Density Functional Theory Study of Chemical Functionalization
of Carbon Nanotubes - Toward Site Selective Functionalization
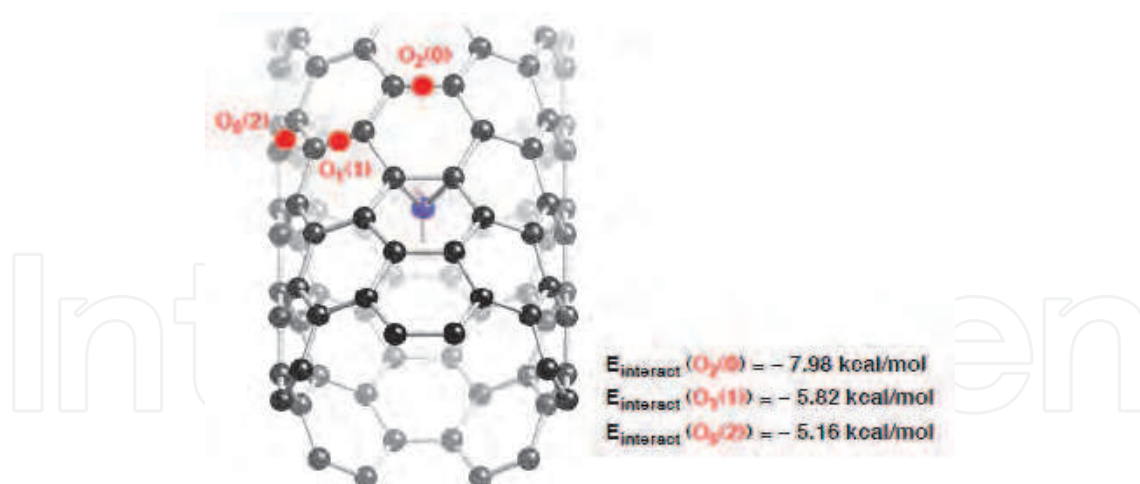
319

Fig. 8. Stable conformations of the binding of the second carbene into the outer surface of the (5,5) nanotube after the first inner addition at an orthogonal bond. The divalent atom of the first attachment is given by blue, and relatively stable sites for the second attachment by blue. The $E_{interact}$ values were obtained from PW91 PBC calculations (Yumura & Kertesz, 2007).

(Yumura & Kertesz, 2007). However, the $E_{interact}$ values are less pronounced than those in the second addition after the first inner addition. Despite negative $E_{interact}$ values at some sites, we found significant positive $E_{interact}$ values at a certain site, meaning that the first carbene prohibits the second carbene from approaching into the sites. Of course, the destabilized effects are due to steric repulsion between the two carbenes. The results suggest that the second carbene cannot bind into a specific CC bond from the others, being in sharp contrast to the inner addition. This is reasonable because Clar patterns of the pristine nanotube remain almost unchanged after the first outer addition.

2.3.2 Site-selective addition of a bismalonate into nanotube

Toward enhancing site-selectivity for the addition of carbene-derivatives into the outer surface of a nanotube, some conformational restrictions of carbene-derivatives would be necessary. To find out a suitable carbene-derivative in this direction, fullerene chemistry can provide helpful hints. Here we pay attention to a successful case of regioselective functionalization of fullerene, reported by Kessinger et al. (Kessinger et al., 2000) They used diethylbutane-2,3-diyl bismalonate as a functional group of fullerene, as shown in Scheme 2. According to their report, a flexible spacer of 2,3-butanediol should be responsible for the selective functionalization. With respect to Bingel reaction, Gao et al. investigated the possible mechanism for the reaction between CCl_3^- and C_{60}, and then compared it with the corresponding carbene reaction mechanism (Gao et al., 2009). According to the B3LYP calculations, both mechanisms are competitive in energy. In addition, Bettinger also analyzed carbene reaction between CCl_2 and a finite-length nanotube, and found that a transition state for the reaction lies only a few kcal/mol above the dissociation limit toward the nanotube and CCl_2 (Bettinger, 2006).

Following the previous experimental and theoretical studies, we recently performed extensive DFT calculations to elucidate the stability of 12 configurations of cycloaddition of diethylbutane-2,3-diyl to the outer surface of a nanotube (Yumura & Kertesz, 2009). Then,
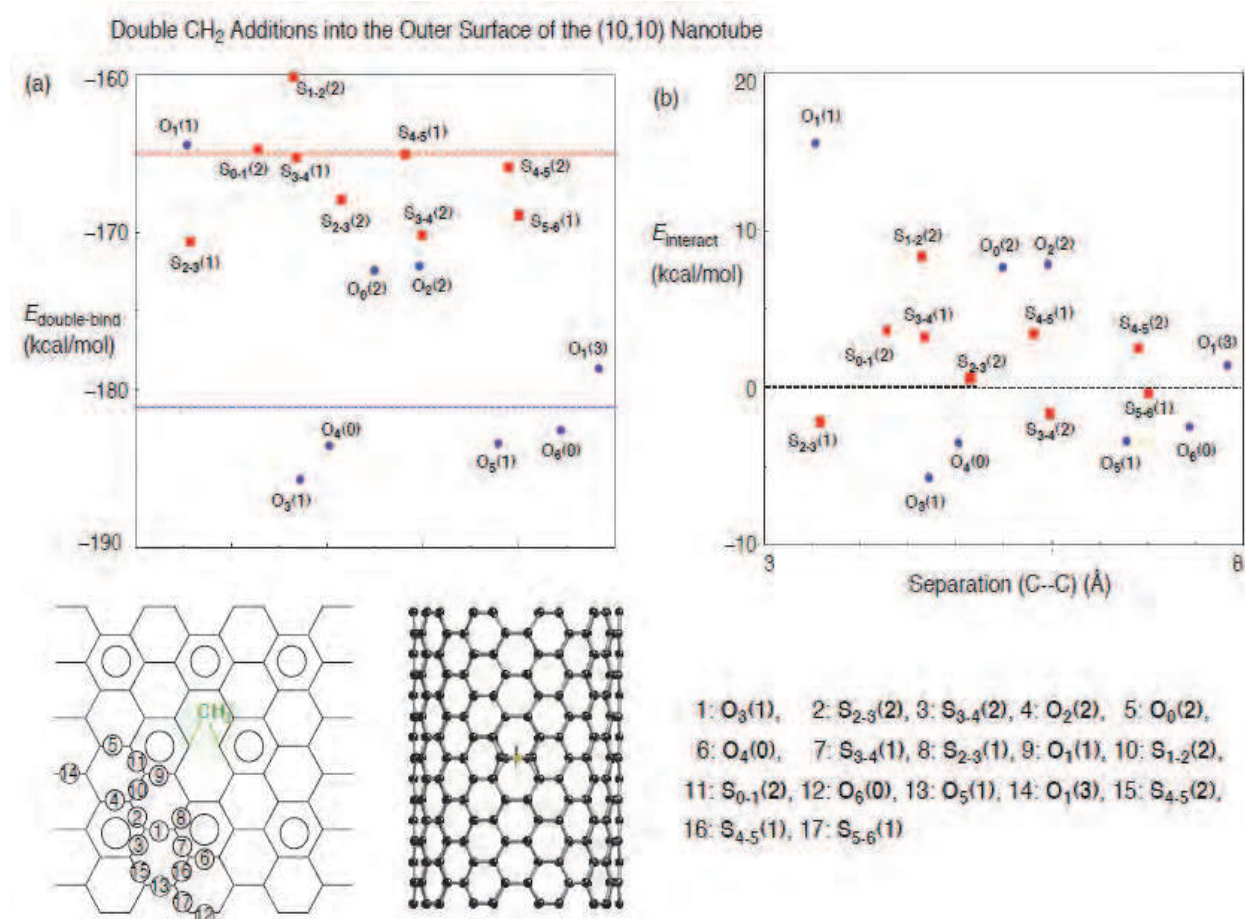
Double CH$_2$ Additions into the Outer Surface of the (10,10) Nanotube

(a) ... (b) ...

Fig. 9. The E$_{double-bind}$ (a) and E$_{interact}$ (b) values in (10,10) nanotube attached by two outer carbenes as a function of the separation between the divalent C11 atoms. Orthogonal additions are given by blue, and slanted additions by red.

we cannot unfortunately obtain a transition state for the carbene mechanism due to computational limitation. In the analysis, we used for simplicity a model of the bismalonate in Chart 1 where terminal Et groups are replaced with the H atoms. DFT calculations found two energetically stable configurations of bismalonate functionalized nanotubes in Figure 10.

The energy difference between the two configurations is 6.5 and 4.7 kcal/mol for the finite-length and infinite-length model calculations, respectively. The energy difference is more pronounced by double addition of outer carbenes. The results suggest that replacement of CH$_2$ by bismalonate enhances site-selectivity of bisfunctionalization of the nanotube.

There are several geometrical factors affecting the binding of a bismalonate with the 2,3-butanediol tether. One of the most important factors is, of course, conformational restriction due to the existence of the 2,3-butanediol tether. The restriction is understandable, because the rotation around the dihedral angle O–C–C–O (θ) of the 2,3-butanediol tether costs energy, as shown in Figure 11 displaying its total energy changes against θ. In fact, Figure 11 shows that there is a barrier of ~5.0 kcal/mol between two local minima in the range of –140 < θ < 140. The rotation of the 2,3-butanediol tether also links to the separation between the two C11 atoms, and thus the tether constraint prohibits the two C11 atoms from freely binding into the nanotube.

A Density Functional Theory Study of Chemical Functionalization
of Carbon Nanotubes - Toward Site Selective Functionalization

321

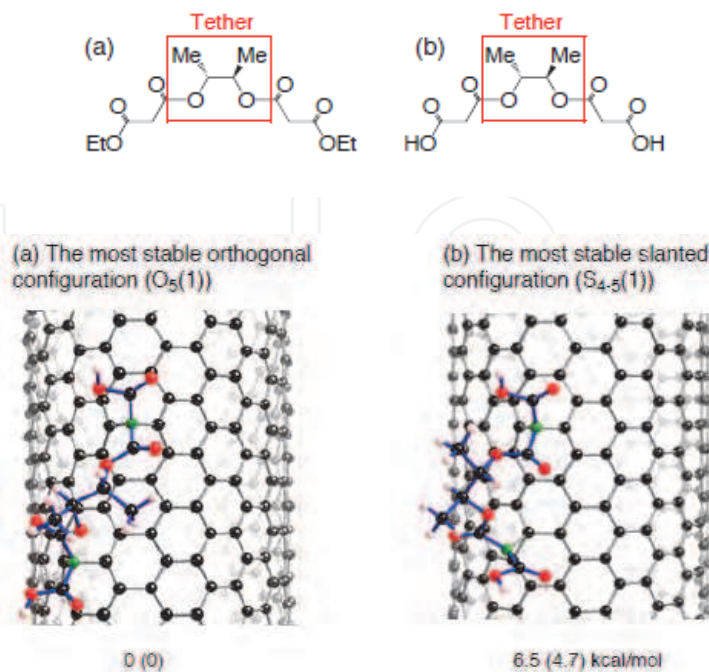Chart 1 Bismalonate with 2,3-butanediol tether and its model.

Fig. 10. Two stable conformations of the binding of the bismalonate with 2,3-butanediol tether into the outer surface of the (10,10) nanotube. The divalent atoms are given by green, oxygen atoms by red, and hydrogen atoms by white. Bonds of the bismalonate are given by blue. The optimized geometries were obtained by PW91 calculation based on PBC and cluster-model approaches. Relative energy obtained from a cluster approach is given, and that from PBC approach in parenthesis (Yumura & Kertesz, 2009).

Another factor differentiating the bismalonate addition from the double carbene addition is that two carboxy substituents affect the aromatic-bismalonate tautomerization in terms of energetics. To look at the importance of binding orientations of carboxy groups, we optimized dicarboxyl-methanononanotube and 11,11-dicarboxy-1,6-methano[10]annulene, where dicarboxycarbene binds into the (10,10) nanotube and naphthalene, respectively. Scanning total energy in 11,11-dicarboxy-1,6-methano[10]annulene along the $d_{1,6}$ bond (Figure 12) indicates that types of the two carboxyl orientations strongly influence the stability of the aromatic and bismalonate forms: double minimum at two carboxyl groups twisted with respect to a mirror plane, whereas single minimum at two carboxyl groups being symmetric.

A different view of Figure 12 suggests that at a longer $d_{1,6}$ bond range, the symmetric form is only available, whereas at a shorter $d_{1,6}$ bond range twisted and symmetric forms are allowed. Thus, the binding orientations (twisted or symmetric forms), determined by the rotation of 2,3-butanediol tether, closely relate with whether the $d_{1,6}$ bond opens or not.

Similar tendencies can be found in the optimized structures for dicarboxy-methanononanotubes. In fact, the optimized structure for the binding of the C11 atom into an orthogonal bond of the (10,10) nanotube has a breaking $d_{1,6}$ bond, and at the same time the two carboxy groups are symmetric, as shown in Figure 13. In contrast, the slanted case with a retaining $d_{1,6}$ bond has a twisted form. Similarly Lee and Marzari found such relationship, and theoretically proposed orientation of two NO_2 groups attached to the C11 atom can control the $d_{1,6}$ bond length on the sp^2 surface of fullerene and a nanotube (Lee & Marzari 2008).
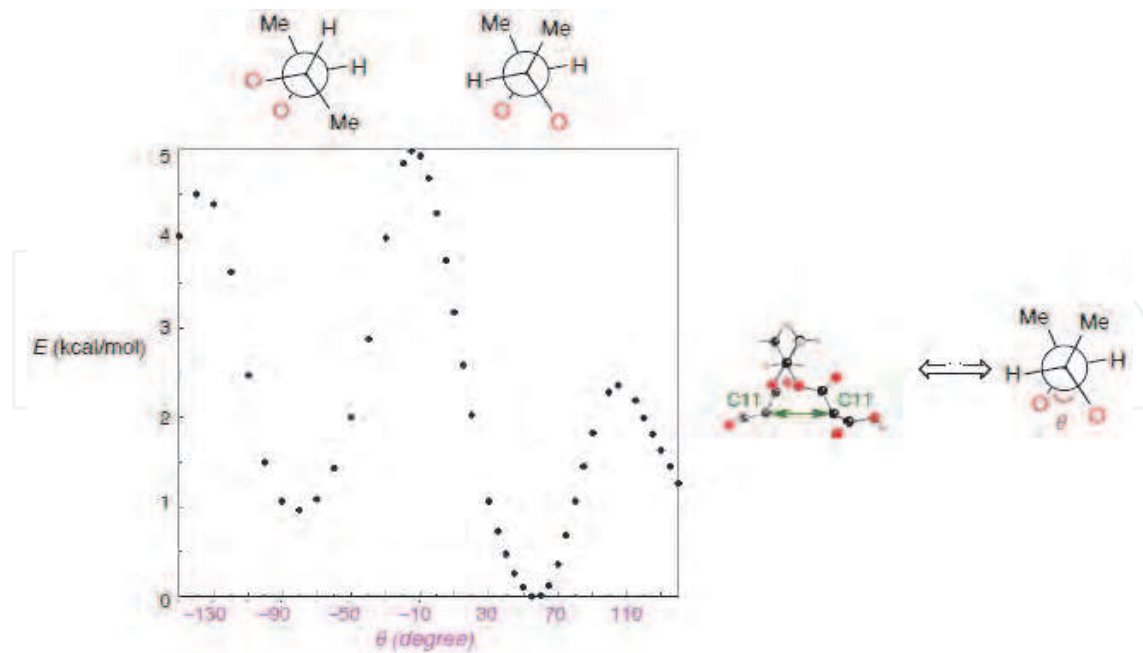
Fig. 11. The energy changes of a free bismalonate with 2,3-butanediol tether upon the rotation around dihedral angle θ of the tether. The energy values were obtained at PW91/6-31G* level of theory (Yumura & Kertesz, 2009).
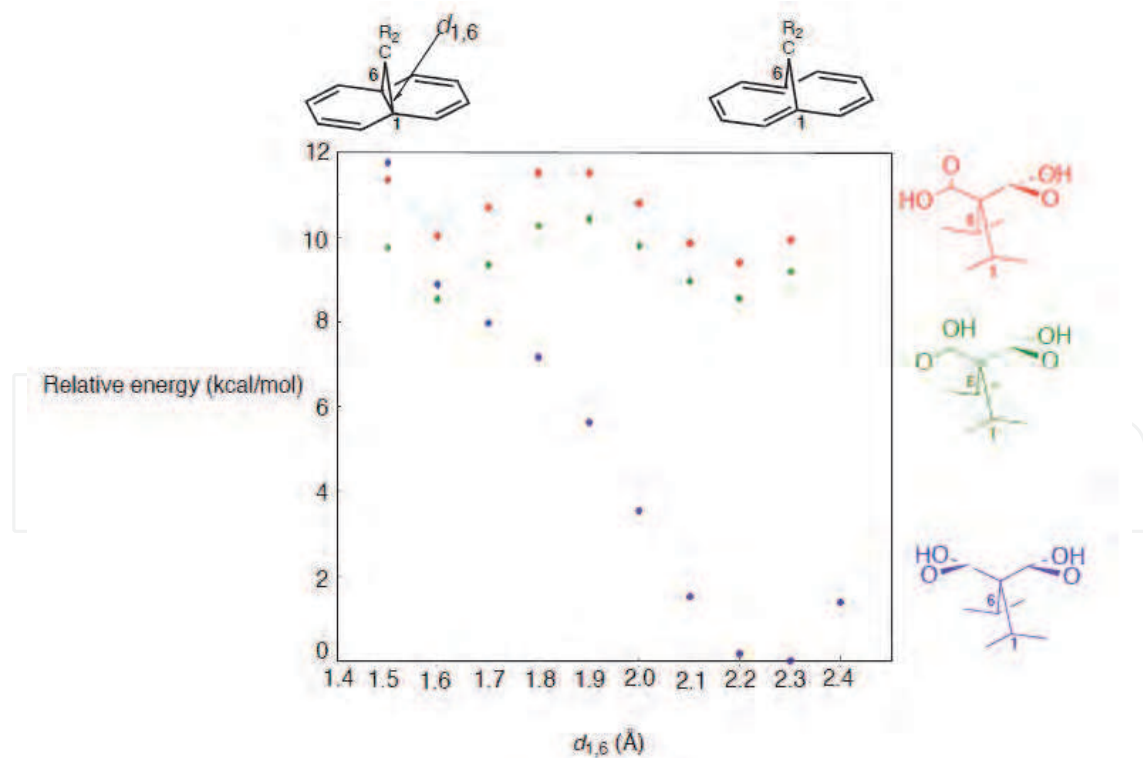

Fig. 12. Total energies of 11,11-dicarboxy-1,6-methano[10]annulene as a function of the $d_{1,6}$ value, obtained at PW91/6-31G* level of theory (Yumura & Kertesz, 2009). In the blue structure, the two carboxy groups are symmetric with respect to a mirror plane, whereas in the green and red structures, the groups are twisted.
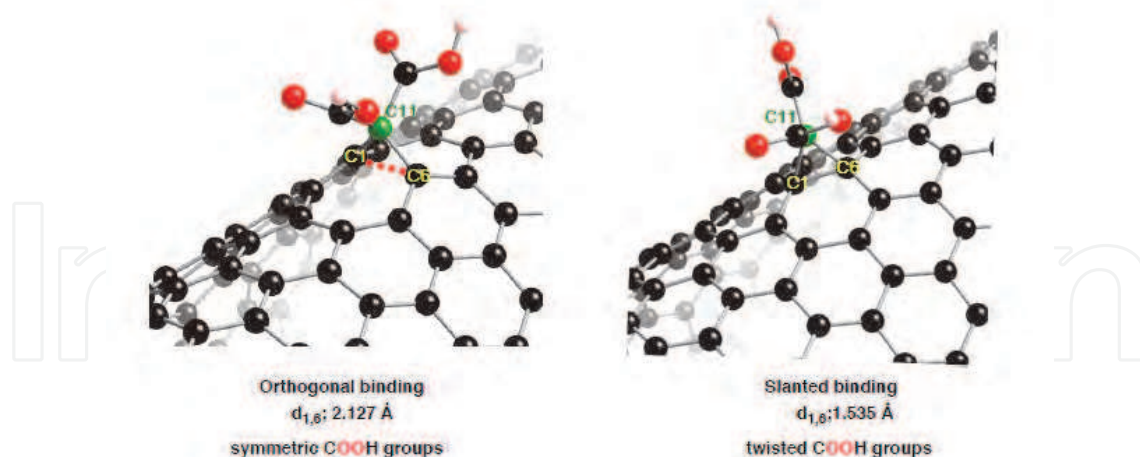
A Density Functional Theory Study of Chemical Functionalization
of Carbon Nanotubes - Toward Site Selective Functionalization

323

Fig. 13. Two types of optimized structure for dicarboxy-methanononanotube. We can distinguish between the two structures by where the divalent C11 atom is bound; an orthogonal or a slanted bond. The divalent atoms are given by green, and oxygen atoms by red. The optimized geometries were obtained by PW91 calculation based on PBC and cluster-model approaches (Yumura & Kertesz, 2009).

Of course, such relationship cannot exist in the double CH_2 addition, and accordingly the binding orientations play a crucial role in the site-selective bismalonate addition. We see quantitatively the effects of the two factors in enhancing the selectivity by estimating the ΔE_{bind} values, given in followings.

$$\Delta E_{bind} = E_{double\text{-}bind} \text{ (bismalonate)} - E_{double\text{-}bind} \text{ (CH}_2) \tag{3}$$

The ΔE_{bind} values are displayed as a function of the separation between the two C11 atoms in Figure 14.
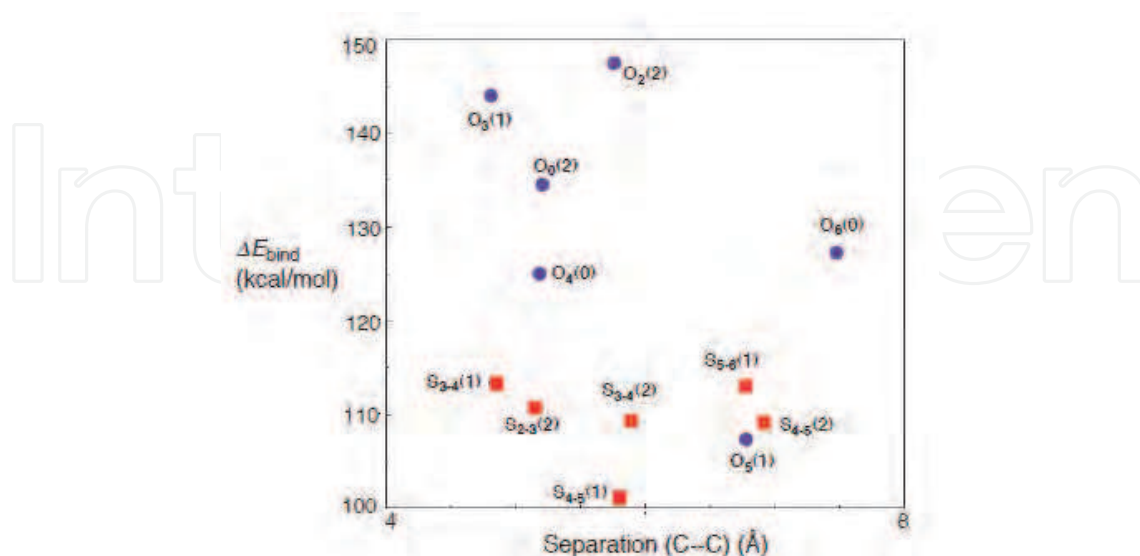

Fig. 14. The differences in the binding energy between the bismalonate and double carbene functionalization (ΔE_{bind}). The ΔE_{bind} values were obtained from a cluster approach at PW91/6-31G*//PW91/3-21G level of theory (Yumura & Kertesz, 2009).

As shown in Figure 14, more significant ΔE_{bind} values were obtained in orthogonal orientations for the second attachment rather than slanted orientations. Since a positive ΔE_{bind} value indicates that a certain orientation is destabilized by the replacement of CH_2 with bismalonate, preferences of an orthogonal site over a slanted site as a second attachment are significantly weakened in the bismalonate functionalization, except for the $O_5(0)$ configuration in Figure 10(a). As a result, site-selectivity can be enhanced by the bismalonate functionalization compared with the double carbene addition (Yumura & Kertesz 2009). The DFT calculations clearly demonstrate that geometrical constraints of carbene derivative are key in the addition of its C11 atoms into a specific sites.

3. Conclusion

Density functional theory (DFT) calculations were employed to devise a plausible strategy for site-selective functionalization of nanotubes by carbene-derivatives. An accurate description of CC bondings of a nanotube functionalized by their divalent carbons was obtained with the aid of large-scale DFT calculations. Then, Clar valence bond (VB) concept, a basic concept in organic chemistry, can help to interpret the disruption of a nanotube surface by carbene-functionalization obtained from DFT calculations, and thus the concept is a useful tool to find out an approach to site-selective functionalization of nanotubes.

The most important DFT finding is that one inner carbene can have the power to locally perturb a nanotube surface by making two covalent bonds. The locally modified surface consists on two butadiene and one quinonoid patterns. In contrast, an outer carbene does not have such power, and accordingly the outer addition cannot disrupt Clar patterns in a pristine nanotube. The differences in the surface modification between the inner and outer bindings originate from whether a CC bond at the binding site opens or not. Note that retaining the CC bond at the binding site for inner carbene is due to more rigorous restriction of surface modification toward the tube center.

Considering different surface modification by the first attachment, we propose two approaches to how functional groups containing a divalent atom can selectively bind into a nanotube. In one approach, one can utilize "local" modification by the first inner attachment to control a site for the second outer attachment. In this situation, the second carbene selectively binds into a CC bond whose electron population enhances upon the first addition. Similar CC bonds with double-bond characters do not emerge on a nanotube functionalized by one outer carbene. Thus geometrical restrictions of a functional group are indispensable for site-selective functionalization of outer surface of a nanotube. For example, a bismalonate with 2,3-butanediol tether is a possible candidate for a functional group that can site-selectively add to a nanotube. For enhancing site-selectivity of functionalization of nanotubes, there are at least two key factors due to geometrical constraints of the bismalonate; a barrier for the rotation around the dihedral angle O–C–C–O of the 2,3-butanediol tether as well as orientations of its carboxy groups attaching divalent atoms. As a result, two divalent atoms of the bismalonate cannot bind freely into a nanotube to enhance the site-selectivity. In the above findings, subtle geometrical changes of nanotube surfaces as well as functional groups are key in site-specific functionalization of nanotubes. Thus, large-scale DFT treatment at relatively accurate manners is required to investigate the nanotube functionalization and to construct nanotube-based building blocks in nano-devices.

A Density Functional Theory Study of Chemical Functionalization
of Carbon Nanotubes - Toward Site Selective Functionalization

325

4. Acknowledgement

5. References

Bahr, J.L. & Tour, J.M. (2001). Highly functionalized carbon nanotubes using in situ generated diazonium compounds. *Chem. Mater.*, 13, 3823-3824.

Bahr, J.L.; Yang, J.; Kosynkin, D.V.; Bronikowski, M.J.; Smalley, R.E. & Tour, J.M. (2001). Functionalization of carbon nanotubes by electrochemical reduction of aryl diazonium salts: A bucky paper electrode. *J. Am. Chem. Soc.*, 123, 6536-6542.

Bahr, J.L.; Mickelson, E.T.; Bronikowski, M.J.; Smalley, R.E. & Tour, J.M. (2001). Dissolution of small diameter single-wall carbon nanotubes in organic solvents? *Chem. Commun.*, 193-194.

Becke, A.D. (1988). Density-functional exchange-energy approximation with correct asymptotic behavior. *Phys. Rev. A*, 38, 3098–3100.

Becke, A.D. (1992). Density-functional thermochemistry. I. the effect of the exchange-only gradient correction. *J. Chem. Phys.*, 96, 2155-2160.

Becke, A.D. (1992). Density-functional thermochemistry. II. the effect of the Perdew-Wang generalized-gradient correlation Correction. *J. Chem. Phys.*, 97, 9173-9177.

Becke, A.D. (1993). Density-functional thermochemistry. III. the role of exact exchange. *J. Chem. Phys.*, 98, 5648-5652.

Bettinger, H.F. (2004). Effects of finite carbon nanotube length on sidewall addition of fluorine atom and methylene. *Org. Lett.*, 6, 731-734.

Bettinger, H.F. (2006). Addition of carbenes to the sidewalls of single-walled carbon nanotubes. *Chem. Euro. J.*, 12, 4372-4379.

Bianchi, R.; Pilati, T. & Simonetta, M. (1980). Structure of 1,6-Methano[10]annulene. *Acta Crystallogr. B*, 36, 3147-3148.

Chen, J.; Hamon, M.A.; Hu, H.; Chen, Y.; Rao, A.M.; Eklund, P.C. & R.C. Haddon, (1998). Solution properties of single-walled carbon nanotubes. *Science*, 282, 95-98.

Chen. Y.; Haddon, R.C.; Fang, S.; Rao, A.M.; Eklund, P.C.; Lee, W.H.; Dickey, E.C.; Grulke, E.A.; Pendergrass, J.C.; Chavan, A.; Haley. B.E. & Smalley, R.E. (1998). Chemical attachment of organic functional groups to single-walled carbon nanotube material. *J. Mater. Res.*, 13, 2423-2431.

Chen, Z.F.; Nagase, S.; Hirsch, A.; Haddon, R.C.; Thiel, W. & Schleyer, P.v.R. (2004). Side-wall opening of single-walled carbon nanotubes (SWCNTs) by chemical modification: A critical theoretical study. *Angew. Chem. Int. Ed.*, 43, 1552-1554.

Chen, Z.F.; Thiel, W. & Hirsch, A. (2003). Reactivity of the convex and concave surfaces of single-walled carbon nanotubes (SWCNTs) towards addition reactions: Dependence on the carbon-atom pyramidalization. *ChemPhysChem*, 4, 93-97.

Choi, C.H. & Kertesz, M. (1998). A new interpretation of the valence tautomerism of 1,6-methano[10]annulene and its derivatives. *J. Phys. Chem. A*, 102, 3429-3437.

Clar, E. (1972). The aromatic sextet; Wiely: London.

Coleman, K.S.; Bailey, S.R.; Fogden, S. & Green, M.L.H. (2003). Functionalization of single-walled carbon nanotubes via the Bingel reaction. *J. Am. Chem. Soc.*, 125, 8722-8723.

Diederich, F. & Thilgen, C. (1996). Covalent fullerene chemistry. *Science*, 271, 317-324.

Dresselhaud, M.S.; Dresselhaus, G. & Eklund, P.C. (1996). Science of fullerenes and carbon nanotubes; Academic Press: San Diego.

Dyke, C.A. & Tour, J.M. (2004). Covalent functionalization of single-walled carbon nanotubes for materials applications. *J. Phys. Chem. A*, 108, 11151-11159.

Gao, X.; Ishimura, K.; Nagase, S. & Chen, Z.F. (2009). Dichlorocarbene addition to C_{60} from the trichloromethyl anion: carbene mechanism or Bingel mechanism? *J. Phys. Chem. A*, 113, 3673-3676.

Globus, A.; Bauschlicher, C.; Han, J.; Jaffe, R.; Levit, C. & Srivastave, D. (1998). Machine phase fullerene nanotechnology. *Nanotechnology*, 9, 192-199.

Goldsmith, B.R.; Coroneus, J.G.; Khalap, V.R.; Kane, A.A.; Weiss, G.A. & Collins, P.G. (2007). Conductance-controlled point functionalization of single-walled carbon nanotubes. *Science*, 315, 77-81.

Haddon, R.C. (1998). Organometallic chemistry of fullerenes: η^2- and η^5-(π)complexes. *J. Comp. Chem.*, 19, 139-143.

Haddon, R.C. (2002). Carbon nanotubes. *Acc. Chem. Res.* 35, 997-997.

Han, J. & Globus, A. (1997). Molecular dynamics simulations of carbon nanotube-based gears. *Nanotechnology*, 8, 95-102.

Hirsch, A. (2002). Functionalization of single-wall carbon nanotubes. *Angew. Chem. Int. Ed.*, 41, 1853-1859.

Hohenberg, P. & Kohn, W. (1964). Inhomogeneous electron gas. *Phys. Rev.*, 136, B864-B871.

Holzinger, M.; Vostrowsky, O.; Hirsch, A.; Hennrich, F.; Kappes, M.; Weiss, R. & Jellen, F. (2001). Sidewall functionalization of carbon nanotubes. *Angew. Chem. Int. Ed.*, 40, 4002-4005.

Iijima, S. (1991). Helical microtubules of graphitic carbon. *Nature*, 354, 56-58.

Iijima, S. & Ichihashi, T. (1993). Single-shell carbon nanotubes of 1-nm diameter *Nature*, 363, 603-605.

Kamarás, K.; Itkis, M.E.; Hu, H.; Zhao, B. & Haddon, R.C. (2003). Covalent bond formation to a carbon nanotube metal. *Science*, 301, 1501-1501.

Kanungo, M.; Lu, H.; Malliaras, G.G. & Blanchet, G.B. (2009). Suppression of metallic conductivity of single-walled carbon nanotubes by cycloaddition reactions. *Science*, 323, 234-237.

Karousis, N.; Tagmatarchis, N. & Tasis, D. (2010). Current progress on the chemical modification of carbon nanotubes. *Chem. Rev.*, 110, 5366–5397.

Kessinger, R.; Thilgen, C.; Mordasini, T. & Diederich, F. (2000). Optically active macrocyclic cis-3 bis-adducts of C_{60}: Regio- and stereoselective synthesis, exciton chirality coupling, and determination of the absolute configuration, and first observation of exciton coupling between fullerene chromophores in a chiral environment. *Helv. Chim. Acta*, 83, 3069-3096.

Kohn, W. & Sham, L. J. (1965). Self-consistent equations including exchange and correlation effects. *Phys. Rev.*, 140, A1133-A1138.

Lee, C.; Yang, W. & Parr, R.G. (1988). Development of the colle-salvetti correlation-energy formula into a functional of the electron density. *Phys. Rev. B*, 37, 785–78.

A Density Functional Theory Study of Chemical Functionalization
of Carbon Nanotubes - Toward Site Selective Functionalization

327

Lee, Y.S. & Marzari, N. (2006). Cycloaddition functionalizations to preserve or control the conductance of carbon nanotubes. *Phys. Rev. Lett.*, 97, 116801.

Lee, Y.S. & Marzari, N. (2008). Cycloadditions to control bond breaking in naphthalenes, fullerenes, and carbon nanotubes: A first-principles study. *J. Phys. Chem. C*, 112, 4480-4485.

Lpez-Bezanilla, A.; Triozon, F.; Latil, S.; Blase, X. & Roche, S. (2009). Effect of the chemical functionalization on charge transport in carbon nanotubes at the mesoscopic scale. *Nano Lett.*, 9, 940-944.

Matsuo, Y.; Tahara, K. & Nakamura, E. (2003). Theoretical studies on structures and aromaticity of finite-length armchair carbon nanotubes. *Org. Lett.*, 5, 3181-3184.

Niyogi, S.; Hamon, M.A.; Hu, H.; Zhao, B.; Bhowmik, P.; Sen, R.; Itkis, M.E. & Haddon, R.C. (2002). Chemistry of single-walled carbon nanotubes. *Acc. Chem. Res.*, 35, 1105-1113.

Ormsby, J.L. & King, B.T. (2004). Clar Valence bond representation of π-bonding in carbon nanotubes. *J. Org. Chem.*, 69, 4287-4291.

Ormsby, J.L. & King, B.T. (2007). The regioselectivity of addition to carbon nanotube segments. *J. Org. Chem.*, 72, 4035-4038.

Park, H.; Zhao, J. & Lu, J.P. (2006). Effects of sidewall functionalization on conducting properties of single wall carbon nanotubes. *Nano Lett.*, 6, 916-919.

Parr, R.G. & Yang, W. (1996). Density-functional theory of atoms and molecules; Oxford University Press: Oxford.

Peng, H.; Alemany, L.B.; Margrave, J.L. & Khabashesku, V.N. (2003). Sidewall carboxylic acid functionalization of single-walled carbon nanotubes. *J. Am. Chem. Soc.*, 125, 15174-15182.

Peng, H.; Reverdy, P.; Khabashesku, V.N. & Margrave, J.L. (2003). Sidewall functionalization of single-walled carbon nanotubes with organic peroxides. Chem. Commn., 362-363.

Perdew, J.P. & Wang, Y. (1992). Accurate and simple analytic representation of the electron-gas correlation energy. *Phys. Rev. B*, 45, 13244.

Prato, M.; Kostarelos, K.; Bianco, A. (2008). Functionalized carbon nanotubes in drug design and discovery. *Acc. Chem. Res.*, 41, 60-68.

Saini, R.K.; Chiang, I.W.; Peng, H.; Smalley, R.E.; Billups, W.E.; Hauge, R.H.; Margrave, J.L. (2003). Covalent sidewall functionalization of single wall carbon nanotubes. *J. Am. Chem. Soc.*, 125, 3617-3621.

Saito, R.; Dresselhaus, G. & Dresselhaus, M.S. (1998). Physical properties of carbon nanotubes.; Imperial College Press: London.

Sato, Y.; Yumura, T.; Suenaga, K.; Urita, K.; Kataura, H.; Kodama, T.; Shinohara, H. & Iijima S. (2006). Correlation between atomic rearrangement in defective fullerenes and migration behavior of encaged metal ions. *Phys. Rev. B*, 73, 233409.

Stevens, J.L.; Huang, A.Y.; Peng, H.; Chiang, I.W.; Khabashesku, V.N. & Margrave, J.L. (2003). Sidewall amino-functionalization of single-walled carbon nanotubes through fluorination and subsequent reactions with terminal diamines. *Nano Lett.*, 3, 331-336.

Stephens, P.J.; Devlin, F.J.; Chabalowski, C.F. & M.J. Frisch, (1994). Ab initio calculation of vibrational absorption and circular dichroism spectra using density functional force fields. *J. Phys. Chem.*, 98, 11623-11627.

Strano, M.S.; Boghossian, A.A.; Kim, W.J.; Barone, P.W.; Jeng, E.S.; Heller, D.A.; Nair, N.; Jin, H.; Sharma, R. & Lee, C.Y. (2009). The chemistry of single-walled nanotubes. *MRS BULLETIN*, 34, 950-961.

Szabo, A. & Ostlund, N,S, (1996). Modern Quantum Chemistry.; Dover Publishing: Mineola, New York.

Tasis, D.; Tagmatarchis, N.; Bianco, A. & Prato, M. (2006). Chemistry of carbon nanotubes. *Chem. Rev.*, 106, 1105-1136.

Umeyama, T.; Tezuka, N.; Fujita, M.; Matano, Y.; Takeda, N.; Murakoshi, K.; Yoshida, K.; Isoda, S. & Imahori, H. (2007). Retention of intrinsic electronic properties of soluble single-walled carbon nanotubes after a significant degree of sidewall functionalization by the Bingel reaction. *J. Phys. Chem. C*, 111, 9734-9741.

Urita, K.; Sato, Y.; Suenaga, K.; Gloter, A.; Hashimoto, A.; Ishida, M.; Shimada, T.; Shinohara, H. & Iijima, S. (2004**)**. Defect-induced atomic migration in carbon nanopeapod: Tracking the single-atom dynamic behavior. *Nano Lett.*, 4, 2451-2454.

Vosko, S.H.; Wilk, L. & Nusair, M. Accurate spin-dependent electron liquid correlation energies for local spin density calculations: a critical analysis**.** (1980). Can. J. Phys. 58, 1200-1211.

Vzquez, E. & Prato, M. (2009). Carbon nanotubes and microwaves: Interactions, responses, and applications. ACS Nano, 3, 3819-3824.

Worsley, K.A.; Moonoosawmy, K.R. & Kruse, P. (2004). Long-range periodicity in carbon nanotube sidewall functionalization. *Nano Lett.,* 4, 1541-1546.

Ying, Y.; Saini, R.K.; Liang, F.; Sadana, A.K. & Billups, W. E. (2003). Functionalization of carbon nanotubes by free radicals. *Org. Lett.*, 5, 1471-1473.

Yumura, T. & Kertesz, M. (2007). Cooperative behaviors in carbene additions through local modifications of nanotube surfaces. *Chem. Mater.*, 19, 1028-1034.

Yumura, T.; Kertesz, M. & Iijima, S. (2007). Confinement effects on site-preferences for cycloadditions into carbon nanotubes. *Chem. Phys. Lett.*, 444, 155-160.

Yumura, T.; Kertesz, M. & Iijima, S. (2007). Local modifications of single-wall carbon nanotubes induced by bond formation with encapsulated fullerenes. *J. Phys. Chem. B*, 111, 1099-1109.

Yumura, T. (2011). Chemically reactive species remain alive inside carbon nanotubes: a density functional theory study. *Phys. Chem. Chem. Phys.*, 13, 337-346.

Yumura, T. & Kertesz, M. (2009). Roles of conformational restrictions of a bismalonate in the interactions with a carbon nanotube. *J. Phys. Chem. C*, 113, 14184-14194.

Zhao, J.J.; Chen, Z.F.; Zhou, Z.; Park, H.; Schleyer, P.v.R. & Lu, J.P. (2005). Engineering the electronic structure of single-walled carbon nanotubes by chemical functionalization. *ChemPhysChem*, 6, 598-601.

Zheng, G.S.; Wang, Z.; Irle, S. & Morokuma, K. (2006). Origin of the linear relationship between $CH_2/NH/O$-SWNT reaction energies and sidewall curvature: armchair nanotubes. *J. Am. Chem. Soc.*, 128, 15117-15126.
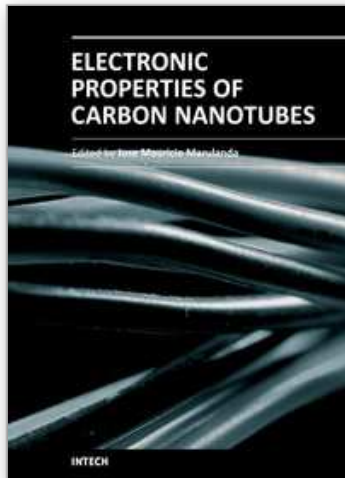
Electronic Properties of Carbon Nanotubes

Edited by Prof. Jose Mauricio Marulanda

Carbon nanotubes (CNTs), discovered in 1991, have been a subject of intensive research for a wide range of applications. These one-dimensional (1D) graphene sheets rolled into a tubular form have been the target of many researchers around the world. This book concentrates on the semiconductor physics of carbon nanotubes, it brings unique insight into the phenomena encountered in the electronic structure when operating with carbon nanotubes. This book also presents to reader useful information on the fabrication and applications of these outstanding materials. The main objective of this book is to give in-depth understanding of the physics and electronic structure of carbon nanotubes. Readers of this book should have a strong background on physical electronics and semiconductor device physics. This book first discusses fabrication techniques followed by an analysis on the physical properties of carbon nanotubes, including density of states and electronic structures. Ultimately, the book pursues a significant amount of work in the industry applications of carbon nanotubes.

How to reference

In order to correctly reference this scholarly work, feel free to copy and paste the following:

INTECH
open science | open minds